Two-Stage Electrohydrodynamic Gas Pump in a Square Channel

A. K. M. M. H. Mazumder and F. C. Lai
School of Aerospace and Mechanical Engineering
University of Oklahoma
phone: 405-325-1748
e-mail: flai@ou.edu

***Abstract*–Earlier studies have shown that an electric field in the form of corona discharge can effectively produce air flow. It has also been shown that an electrohydrodynamic (EHD) gas pump can produce gas flows with a maximum velocity of 5 m/s. Its maximum performance of 35 L/s/W is better than that of conventional cooling fans used in personal computers. In this study, an EHD pump with two-stage, each stage with a 28 emitting electrodes, is tested for a wide range of operating voltages starting from the corona threshold voltage up to 28 kV for further improvement in its performance. To seek the relation between the pump performance and number of stages, the EHD gas pump is critically evaluated by experimental measurements and numerical simulations. The maximum performance of 34 L/s/W is achieved by using total 56 electrodes with 0.5 inch wide grounded plate in each stage.**

INTRODUCTION

A subject of great interest for many years is the use of electrical field to enhance heat and mass transfer. This enhancement mechanism is based on the use of an electrical body force to induce a secondary flow or simply create a flow where none would otherwise exist. Corona discharge usually involves two asymmetric electrodes; one highly curved (such as the tip of a needle, or a small diameter wire) and one of low curvature (such as a plate). The high curvature ensures a high potential gradient around the electrode. A corona discharge occurs in the narrow region close to the highly curved electrode and gas molecules are ionized by a high electrical field. Controlled by Coulomb force, these ions migrate to the grounded electrode. These ions transfer their momentum to neutral molecules via collision during the migration to the grounded electrode. This creates a bulk flow, which is usually called ionic wind, or corona wind [1]. Corona wind is produced by an electrode charged with a direct current (positive or negative) at a sufficiently high voltage (in the kV range). While the applied voltage may be high, the current involved is usually very small (in the μA to mA range), which makes the power required considerably insignificant. This has become one of the most attractive features for electrohydrodynamic (EHD) technique. In recent years, there has been a surge of interest in the application of EHD technique for pumping dielectric liquids [2]. Because

of their low power consumption and no moving part, EHD pumps have been considered a valuable alternative for conventional pumps.

Electrohydrodynamic flows have been applied to wide engineering fields. For example, in the food industry, corona wind has become a novel drying method to enhance the dehydration process [3-5]. EHD actuators are used in the aerospace industry to reduce the drag of an aircraft or to stabilize the air flow [6-10]. In the thermal management of electronic systems, corona wind can produce a substantial increase in the heat transfer coefficient [11-13], which is also referred to as the electrohydrodynamic (EHD) enhancement technique. In addition, EHD technique has been widely used in manufacturing and power industries (i.e., electrostatic precipitators) to control particle emission and increase the efficiency of particle collection [14]. Recently, as microelectronics has become an emerging technology, EHD techniques have played an important role in the development of microelectromechanical system (MEMS) [15].

Electrohydrodynamic technique has many advantages. Firstly, this technique directly converts electric energy into kinetic energy without involving moving mechanical parts, and therefore the maintenance cost can be greatly reduced. Secondly, this technique is operated electronically and it may be incorporated into the existing systems to be conveniently controlled by a computer. Thirdly, it is highly compatible with chips and chip-level structures. Thus, miniaturization can be easily implemented [16]. Lastly and most importantly, the power consumption is usually very small, which makes this technique particularly attractive from the energy point of view. Its only disadvantage is the generation of extraneous gases such as ozone that might be harmful to human beings. However, ozone generation can be effectively monitored and minimized [17].

Rickard, et al. [18] investigated the characteristics of ionic wind velocity in a tube with a pin-to-ring electrode geometry for negative corona discharge. In addition, they added a converging nozzle to the exit of the tube with an intention to accelerate the gas flow produced by the ionic wind generator. However, they found that only a slight increase in the velocity was achieved by using the converging nozzle. A wire-non-parallel-plate EHD gas pump was experimentally investigated by Tsubone, et al. [19]. A maximum air velocity of 1.9 m/s, which corresponds to a volumetric flow rate of 44 L/min, was observed. The volumetric flow rate, gas velocity and pressure drop were found to increase with increasing applied voltage or EHD number. Also, their numerical results [20] agreed qualitatively well with their experimental data. The flow characteristics of a wire-rod type EHD gas pump were studied by Komeili, et al. [21] for various pipe diameters. Experiments were conducted using negative corona discharge with applied voltage ranging from 0 to 24 kV. A maximum gas flow rate of 40.1 L/min was generated for a pipe diameter of 20 mm, with a grounded rod electrode of a diameter of 3.1 mm and an electrode spacing of 12.6 mm. Their results showed that for the same pipe diameter and electrode spacing, the velocity generated increased with the rod diameter. However, they suggested that for a fixed gas velocity it was better to use a rod electrode with a smaller diameter as it would generate the same flow velocity for lower power consumption. The efficiency of an EHD gas pump with a grid-and-ring grounded electrode has been experimentally evaluated by Moreau and Touchard [22]. Their results showed that positive

coronas could produce a higher air velocity than negative ones. Using a grid as the collecting electrode was more efficient than a ring. In their experiments, they were able to produce a corona wind of 10 m/s and a flow rate of about 1 L/s. Jewell-Larsen et al. [23] reported that electrostatic air propulsion is a promising technology with such potential applications as energy-efficient ventilation, air sterilization, cooling of electronics, and dehumidification. They found that the challenges of existing designs include the need to increase airspeed, backpressure, energy efficiency, and heat exchange capability. They conducted this study for the purpose of optimizing device characteristics through the control of the electric field distribution.

Although EHD gas pumps are promising, there are still some challenging questions to be addressed. The first is associated with the high voltage required to drive the flow in a large scale system. However, it is expected that the operating voltage will decrease as the scale of the system is reduced, thus promoting its use in microsystems. In fact, the implementation of EHD pumping has received tremendous attention lately due to an increasing interest in microfluidics, chip-integrated cooling, and drug delivery systems [24]. Although EHD gas pumps are effective in delivering and transport of gas, it has been observed that their effect may be confined to a short range [25]. It has been speculated that using a two-stage EHD gas pump may help solving the problem. One is to initiate the flow and the other to further accelerate the flow. Thus the objective of the present study is to address this important issue in the EHD gas pump design. To aid the investigation, experimental measurements and numerical simulations have been conducted.

EXPERIMENTAL SETUP, NUMERICAL FORMULATION AND PROCEDURE

A. Experimental Setup

The schematic of the experimental setup used in this study is shown in Fig. 1. The main components are: EHD pump test unit, high voltage power supply, air velocity transducer, and data acquisition system (DAQ). The test channel was constructed from Plexiglas of ¼ inch thick. The inner dimensions of the channel were 4 inches by 4 inches with a length of 30 inches. The dimensions of the wire-electrode and system configuration are shown in Fig. 2. A copper wire of 20 GA (0.03196 inch diameter) was first bent and welded to form the electrode loop flush mounted on the inner wall of the channel. Additional one-inch-long copper wires of the same size were welded to the base loop to serve as emitting electrodes. A 0.5-inch wide and 0.025 inch thick copper strip at each stage was also flush mounted on all four sides of the inner wall and served as the grounded electrode. The gap between the tips of the emitting electrodes and the grounded plate was maintained at 1.5 inches for each stage. The gap between the electrode wire loops of top stage to bottom stage was maintained at 6 inches. It is necessary to include the wire pins to create a non-uniform electric field to produce corona wind. The emitting electrode pins were evenly distributed over the channel walls. The electrode assembly and the grounded plate were press-fitted to pre-cut grooves on the inner wall of the channel so that their surfaces were flushed with the channel wall. In this arrangement, the corona wind produced by the electrode will resemble that of a wall jet. Also, the emitting electrodes were intended to align with the direction of primary flow to maximize its effect of.

The wire electrode assembly was connected to a high voltage (max. 30 kV) power supply (Bertan Associates, Series 205B-30R) and charged with a direct current of either positive or negative polarity. The plate was grounded at the same level of the powersupply. Two ¼ inch NPT compression fittings were installed on the lower part (outlet section) of the channel to hold the velocity transducer (Omega FMA 902-I) in place to facilitate air flow measurements. The transducer, which can accurately measure air velocity from 0 to 500 fpm (2.54 m/s) with an accuracy of 2.7% of full scale at room temperature. The velocity probe extended horizontally from channel wall allowing measurements be taken on three levels; 1, 2.5 and 4 inches downstream of the grounded plate of the bottom stage. A total of twenty one sampling points are evenly distributed on each level. The data acquisition system used is from National Instruments. The data sampling and collection are aided by the LabView program. The current signal received from the power supply and the velocity transducer are first calibrated and scaled to the correct current and

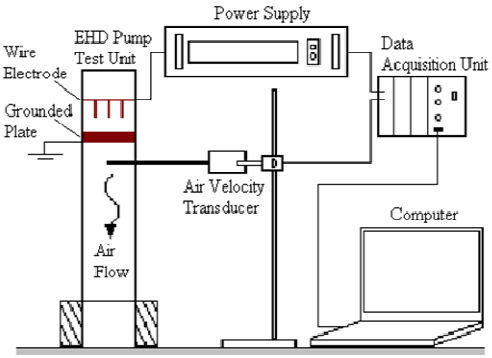

Fig. 1 Schematic of the experimental setup.

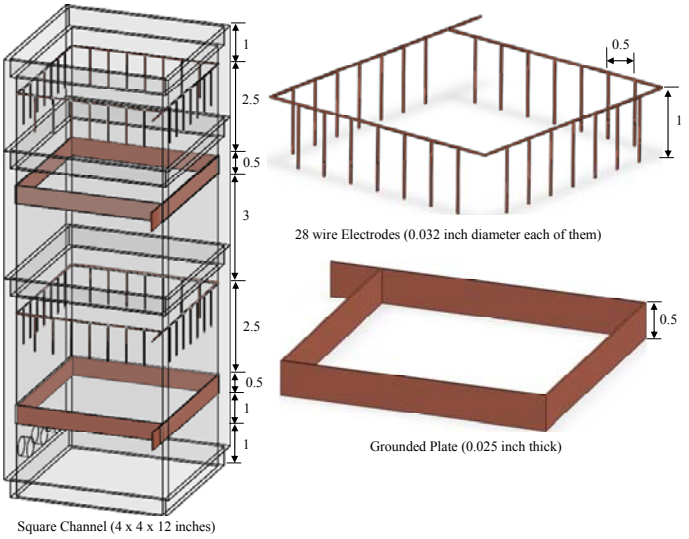

Fig. 2 Configuration of EHD pump test unit.

air velocities. A sampling rate of 1 Hz is used for all experiments. It is determined by systematic trials that 1 Hz is sufficient to capture the variations of electric and flow fields.

Experiments are conducted with only positive corona discharge in this study. Negative polarity will be considered in the future for comparison. To start the experiment, the applied voltage was gradually increased until a flow was detected by the velocity transducer. For the present setup, corona wind was too weak to be detected until the applied voltage was increased to 20 kV. The applied voltage was then incrementally increased by two kilovolts until sparkover occurred, which could be easily observed through a visible bright light and cracking sound that it produced. When it occurred, electric field became unstable and fluctuates violently. As such, it should be avoided to operate beyond this voltage. Typical V-I curves for the present experimental setup are shown in Fig. 3. As seen, the current produced by corona discharges increases with the applied voltage after the onset of corona.

B. Numerical Formulation and Procedure

For the problem considered, the governing equations in Cartesian coordinates for the electrical field are given by Zhang and Lai [25],

$$\frac{\partial^2 V}{\partial x^2}+\frac{\partial^2 V}{\partial y^2}+\frac{\partial^2 V}{\partial z^2}=-\frac{\rho_c}{\varepsilon}, \tag{1}$$

$$\frac{\partial \rho_c}{\partial x}\frac{\partial V}{\partial x}+\frac{\partial \rho_c}{\partial y}\frac{\partial V}{\partial y}+\frac{\partial \rho_c}{\partial z}\frac{\partial V}{\partial z}=\frac{\rho_c^2}{\varepsilon}, \tag{2}$$

which can be derived from Maxwell equation, current continuity equation and Ohm's law. Owing to the symmetry of the problem, only one quarter of the channel was needed for computations. Thus, the corresponding boundary conditions for the electric field are,

At the wire, $V = V_0.$ (3a)

At the grounded plate, $V = 0.$ (3b)

At the inlet and outlet, $\frac{\partial V}{\partial z} = 0$ (3c)

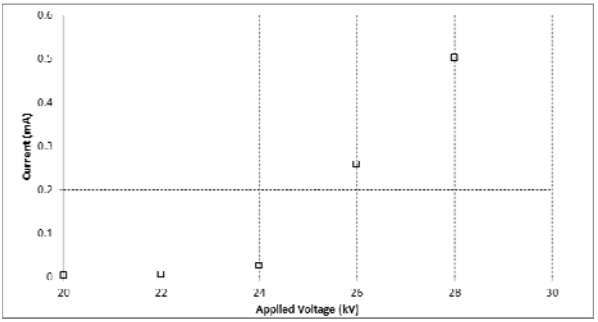

Fig. 3 Typical V-I curves for EHD gas pumps with two stages of electrodes.

On the channel walls except the grounded plate,

$$x = 0, \qquad \frac{\partial V}{\partial x} = 0. \tag{3d}$$

$$y = 0, \qquad \frac{\partial V}{\partial y} = 0. \tag{3e}$$

On the symmetric surfaces,

$$x = \frac{D}{2}, \qquad \frac{\partial V}{\partial x} = 0. \tag{3f}$$

$$y = \frac{D}{2}, \qquad \frac{\partial V}{\partial y} = 0. \tag{3g}$$

Computations for the electric field have been performed using an in-house program based on the finite different method. The EHD gas pump has actual dimensions of 4 by 4 by 30 inches. For the electric field calculations, it is anticipated that the electric field does not vary further downstream of the grounded plate. As such, a channel length of 16 inches has been has been used in the numerical model to reduce the computational time. A uniform grid of 51 x 51 x 401 has been selected for the present calculations. Since the radius of the electrode wire is very small, it is appropriate to treat the wire as a nodal point. For the solution of electric field, a numerical procedure proposed by Yamamoto and Velkoff [14] has been employed. In this procedure, electric potential and space charge density are determined by iterations on Eqs. (1) and (2) with an assumed value of space charge density at the wire tip (ρ_{c0}). The validity of the solution is checked by comparing the predicted total current (Eq. (4)) with the measured experimental current at the corresponding voltage. If the currents do not match, a new value of space charge density at the wire tip is assumed and the calculations are repeated until the calculated total current agrees well with the measure value for that given applied voltage. There are other algorithms for the solution of electric field (e.g., those proposed by McDonald et al. [26] as well as Kalio and Stock [27]), in which the electrical field condition at the wire is estimated by the Peek's semi-empirical formula [28] instead of an assumed value. It should be pointed out that an empirical constant, named the wire condition factor, has been introduced in the formula mentioned above. Since the assignment of this empirical constant is somewhat arbitrary, we prefer the approach proposed by Yamamoto and Velkoff [14] over the later ones [26-27]. However, it has been reported [29-30] that the agreement between the results obtained by these two approaches is very good when the solutions converged.

$$I_{cal} = 2\int_0^D \int_0^W \rho_c b E_x \, dydz + 2\int_0^D \int_0^W \rho_c b E_y \, dxdz, \tag{4}$$

When this calculated current agrees well with the experimental data (i.e., to satisfy Eq. (5)), the electric field is considered converged.

$$\left| \frac{I_{cal} - I_{exp}}{I_{cal}} \right| \le 10^{-3} . \tag{5}$$

Computations have been performed on a 64-bit workstation with a 2 GHz CPU and 8 Gb of RAM. A typical run takes about seven hours of CPU time for the solution of the electric field.

RESULTS AND DISCUSSION

The electric potential distributions inside the test channel are shown in Fig. 4 for an EHD gas pump with applied voltage varying from 20 kV to 28 kV at an increment of 2 kV. The potentials displayed in the figure have been normalized with the voltage applied at the wire. It is observed that a large potential gradient exists between the wire electrodes and the grounded plate for both top and bottom stages. The electric potential is slightly higher in the core region of the channel than that on the channel surface. Below the grounded plate of the bottom stage, the potential does not vary significantly. Hence, it is justified to use a shorter channel length for the electric field calculations. From Fig. 4, one can see that the electrode pins has significantly modified the electric field. This non-uniform electric field is an essential condition for the generation of corona wind.

Space charge density distributions are shown in Fig. 5 for an EHD gas pump with the same applied voltages. The charge density displayed is also normalized with its value at the electrode tips. As observed, space charges are centered around the electrode tips and spread downwards to the grounded plate at both top and bottom stages. Their density reduces significantly when moving away from the wire tip. With an increase in the applied voltage, space charges are further confined to a smaller region at the tip. It is interesting to observe that space charges fill up the entire region between the electrode tips and the grounded plate as a lower voltage. However, at an applied voltage of 26 kV and 28 kV, space charges are highly concentrated at the electrode tips, and their density reduces dramatically within a short distance away from the tips.

Figure 6 depicts the velocity profile inside the channel. In this figure, the x- axis represents the channel width so that the locations of x = 0 and x = 4 inch refer to the channel

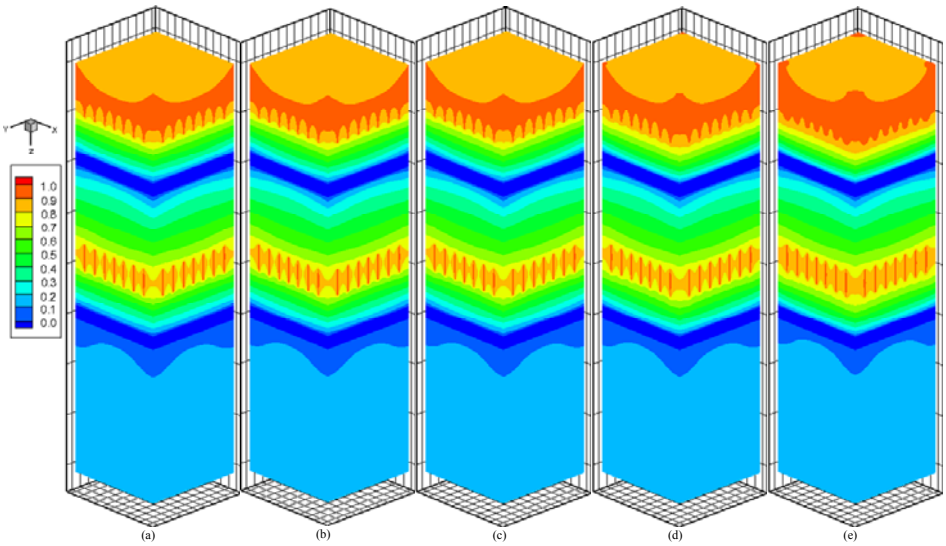

Fig. 4 Electric potential distribution in an EHD gas pump with various applied voltage, (a) V_o = 20 kV, (b) V_o = 22 kV, (c) V_o = 24 kV, (d) V_o = 26 kV, (e) V_o = 28 kV.

walls. The velocity profile looks like an inverted parabola, which is the opposite of a fully developed velocity profile for forced flows inside a channel. This is mainly due to the fact that the emitting electrode was embedded in the channel wall. The corona wind produced by these electrodes behaves like a wall jet, leading to the maximum air velocity occurring near the wall. This feature is more pronounced when the applied voltage increases ($V_o \geq 24$ kV). However, when the applied voltage is low ($V_o = 20$ kV), the velocity profile is fairly uniform across the channel. Although one would anticipate a symmetrical velocity profile, one observes that the velocity at x = 0.5 in. is actually higher than that at x = 3.5 in. This asymmetric velocity profile is caused by the presence of the velocity measuring probe, which has adversely disturbed the flow. In addition, the induced airflow velocity increases with an increase in the applied voltage. The highest velocity measured in this configuration is as high as 1.5 m/s. These velocities are measured at the cross-section z = 1 in. downstream from the grounded plate at the bottom stage. The same features hold for other cross-section levels (z = 2.5 inch and z = 4 inch).

The average volume flow rate of air induced by the EHD gas pump is shown in Fig. 7 as a function of applied voltage. The induced volume flow rate of air increases with an increase in the applied voltage. The maximum volume flow rate observed in this study is 10.5 L/s at a given applied voltage 28 kV. To evaluate the performance of EHD gas pump proposed, an energy efficiency rating is employed, which is defined as the amount of air volume flow rate delivered per wattage of electric power consumed. The unit for this rating is usually CFM/W (cubic feet per minute per watt) or L/s/W (liters per second per watt).

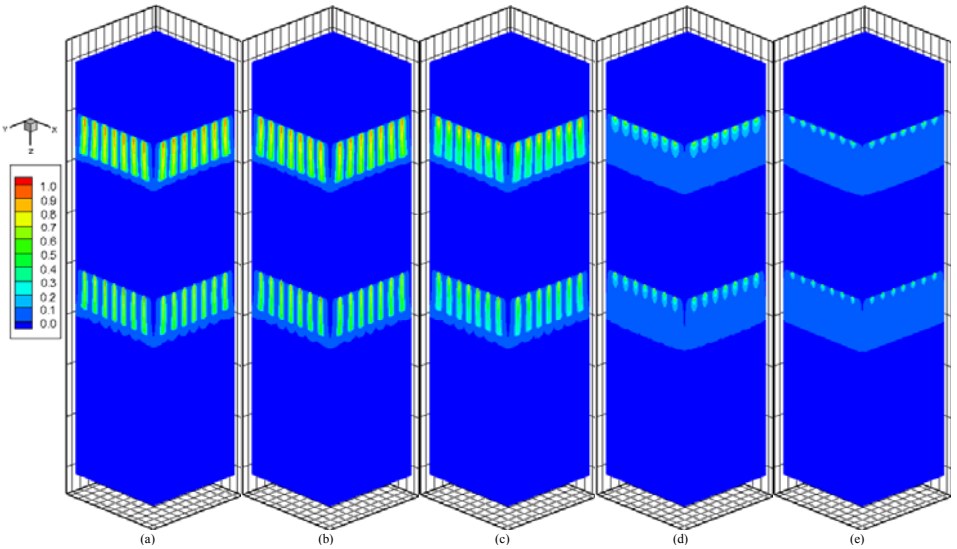

Fig. 5 Space charge density distribution in an EHD gas pump different applied voltage, (a) $V_o = 20$ kV, (b) $V_o = 22$ kV, (c) $V_o = 24$ kV, (d) $V_o = 26$ kV, (e) $V_o = 28$ kV.

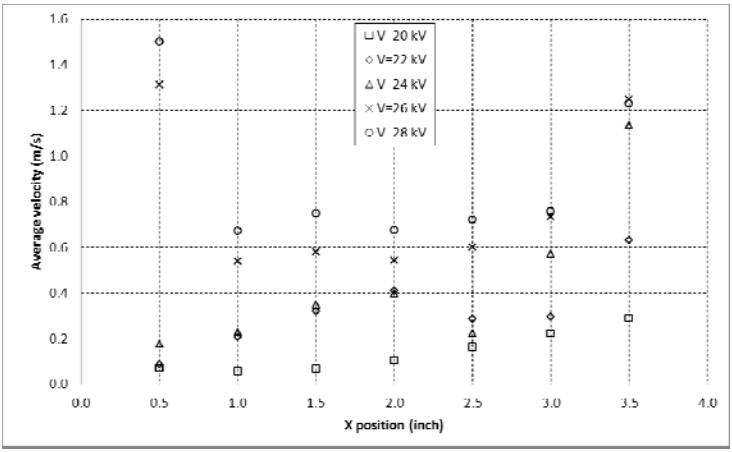

Fig. 6 Velocity profiles inside the channel at 1 inch downstream from the grounded plate of the bottom stage.

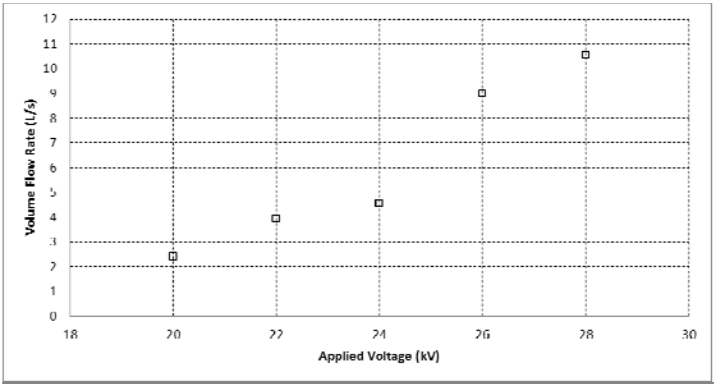

Fig. 7 Average volume flow rate as a function of applied voltage.

Figure 8 shows the EHD gas pump performance as a function of the applied voltage. The gas pump has a maximum performance of 34 L/s/W operated at an applied voltage of 20 kV. The performance decreases sharply as the applied voltage increases. The performance of conventional computer cooling fans ranges from 1 to 4 L/s/W as reported by Jewell-Larsen et al. [23], which is considered low when comparing with the data shown in Fig. 8. The EHD gas pump studied in the present study appears to be more effective in terms of energy usage. In addition, with no moving parts, the EHD gas pump can offer much quieter operation than the conventional fans.

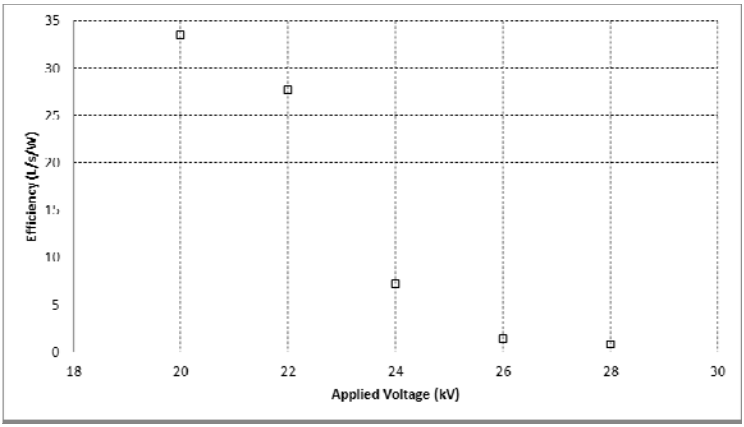

Fig. 8 Performance of two-stage EHD gas pump as a function of applied voltage.

CONCLUSION

Experimental and numerical studies have been performed for a two-stage electrohydrodynamic (EHD) gas pump operated by positive corona discharge. Some numerical results have been obtained for the electric field in the EHD gas pump. The electric potential and space charge distributions have been visually examined at various applied voltages. Visualizations from numerical results reveal that corona wind issued from the electrodes behaves like a set of wall jets, leading to high velocity gradients near the channel walls. It has been shown that the induced air velocity increases with an increase in the applied voltage. Since the electrode pins are mounted on the inner surface of the channel wall, corona wind issued from the electrodes behaves like a set of wall jets, resulting in an inverted parabolic velocity profile at the center of the channel with the maximum velocity close to the channel wall. The maximum volume flow rate of air induced by the proposed EHD gas pump is as high as 10.5 L/s operating at a voltage of 28 kV. Depending on the application, an applied voltage can be selected to achieve the desired outcome. As far as the performance is concerned, it has been shown that the EHD gas pump proposed is more effective than most conventional fans. Depending on the application, the present EHD pump can be further tailored (in terms of electrode configuration and applied voltage) to achieve the desired outcome.

NOMENCLATURE

b	ion mobility of air
D	channel width
E_x	electric field strength in x-direction
E_y	electric field strength in y-direction
E_z	electric field strength in z-direction
I_{cal}	numerically calculated corona current
I_{exp}	experimentally measured corona current
L	length of channel
V	electric potential

V_0 applied voltage at the wire
$\overline{v}$ normalized electric potential, = V/V_0
W width of the grounded plate
x, y, z Cartesian coordinates
ε permitivity of air
ρ_c space charge
ρ_{c0} space charge at the wire tip
$\overline{\rho_c}$ normalized space charge, = ρ_c/ρ_{c0}

REFERENCES

[1] M. Robinson, "Movement of air in the electric wind of the corona discharge," *Transactions of the American Institute of Electrical and Electronic Engineers,* vol. 80, pp. 143-150, 1961

[2] J. Seyed-Yagoobi, Electrohydrodynamic Pumping of Dielectric Liquids, *Journal of Electrostatics*, vol. 63, pp. 861-869, 2005.

[3] F. C. Lai and K. W. Lai, "EHD-enhanced drying with wire electrode," *Drying Technology,* vol. 20, pp. 1393-1405, 2002.

[4] A. Alem-Rajabi and F. C. Lai, "EHD-enhanced drying of partially wetted glass beads," *Drying Technology,* vol. 23, pp. 597-609, 2005.

[5] T. I. J. Goodenough, P. W. Goodenough, and S. M. Goodenough, "The efficiency of corona wind drying and its application to the food industry," *Journal of Food Engineering,* vol. 80, pp. 1233-1238, 2007.

[6] L. Leger, E. Moreau, G. Artana, and G. Touchard, "Influence of a DC corona discharge on the airflow along an inclined flat plate," *Journal of Electrostatics,* vol. 51, pp. 300-306, 2001.

[7] R. Vilela Mendes and J. Dente, "Boundary-layer control by electric fields: A feasibility study," *Journal of Fluids Engineering-Transactions of the ASME,* vol. 120, pp. 626-629, 1997.

[8] E. Moreau, G. Artana, and G. Touchard, "Surface corona discharge along an insulating flat plate in air applied to electrohydrodynamically airflow control: electrical properties," *Electrostatics Conference*, vol. 178, pp. 285-290, 2004.

[9] E. Moreau, L. Léger, and G. Touchard, "Effect of a DC surface-corona discharge on a flat plate boundary layer for air flow velocity up to 25 m/s," *Journal of Electrostatics,* vol. 64, pp. 215-225, 2006.

[10] P. Magnier, D. Hong, A. Leroy-Chesneau, J. M. Pouvesle, and J. Hureaua, "A DC corona discharge on a flat plate to induce air movement," *Journal of Electrostatics,* vol. 65, pp. 655-659, 2007.

[11] M. M. Ohadi, D. A. Nelson, and S. Zia, "Heat-transfer enhancement of laminar and turbulent pipe-flow via corona discharge," *International Journal of Heat and Mass Transfer,* vol. 34, pp. 1175-1187, 1991.

[12] M. Molki, M. M. Ohadi, B. Baumgarten, M. Hasegawa, and A. Yabe, "Heat transfer enhancement of airflow in a channel using corona discharge," *Journal of Enhanced Heat Transfer,* vol. 7, pp. 411-425, 2000.

[13] M. Molki and P. Damronglerd, "Electrohydrodynamic enhancement of heat transfer for developing air flow in square ducts," *Heat Transfer Engineering,* vol. 27, pp. 35-45, 2006.

[14] T. Yamamoto and H. R. Velkoff, "Electrohydrodynamics in an electrostatic precipitator," *Journal of Fluid Mechanics,* vol. 108, pp. 1-18, 1981.

[15] A. Richter, A. Plettner, K. A. Hofmann, and H. Sandmaier, "A micromachined electrohydrodynamic (EHD) pump," *Sensors and Actuators a-Physical,* vol. 29, pp. 159-168, 1991.

[16] L. Tanasomwang and F. Lai, "Long-term ozone generation from electrostatic air cleaners," *Conference Records of the 1997 IEEE Industry Applications Society 32nd IAS Annual Meeting*, vol. 3, pp. 2037-2044, 1997.

[17] L. Fouad and S. Elhazek, "Effect of humidity on positive corona discharge in a 3-electrode system," *Journal of Electrostatics,* vol. 35, pp. 21-30, 1995.

[18] M. Rickard, D. Dunn-Rankin, F. Weinberg, and F. Carleton, "Characterization of Ionic Wind Velocity," *Journal of Electrostatics,* vol. 63, pp. 711-716, 2005.

[19] H. Tsubone, J. Ueno, B. Komeili, S. Minami, G. D. Harvel, K. Urashima, C. Y. Ching, and J. S. Chang, Flow Characteristics of Wire-non-parallel Plate Electrohydrodynamic Gas Pumps, *Journal of Electrostatics,* vol. 66, pp. 115-121, 2008.

[20] J. S. Chang, H. Tsubone, Y. N. Chun, A. A. Berezin, and K. Urashima, Mechanism of Electrohydrodynamically Induced Flow in a Wire-non-parallel Plate Electrode Type Gas Pump, *Journal of Electrostatics,* vol. 67, pp. 335-339, 2009.
[21] B. Komeili, J. S. Chang, G. D. Harvel, C. Y. Ching, and D. Brocilo, Flow Characteristics of Wire-rod Type Electrohydrodynamic Gas Pump under Negative Corona Operations, *Journal of Electrostatics,* vol. 66, pp. 342-353, 2008.
[22] E. Moreau and G. Touchard, Enhancing the Mechanical Efficiency of Electric Wind in Corona Discharges, *Journal of Electrostatics,* vol. 66, pp. 39-44, 2008.
[23] N. E. Jewell-Larsen, I. A. Krichtafovitch, and A. V. Mamishev, "Design and Optimization of Electrostatic Fluid Accelerators," *IEEE Transactions on Dielectrics and Electrical Insulation,* vol. 13, pp. 191-203, 2006.
[24] D. J. Laser and J. G. Santiago, A Review of Micropumps, *Journal of Micromechanics and Mircoengineering*, vol. 14, pp. R35-R64, 2004.
[25] J. Zhang and F. C. Lai, "Effect of Emitting Electrode Number on the Performance of EHD Gas Pump in a Rectangular Channel," *Proceedings of the Electrostatics Society of America (ESA) Annual Meeting 2010.*
[26] J. R. McDonald, W. B. Smith, H. W. Spencer and L. E. Sparks, "A Mathematical Model for Calculating Electrical Conditions in Wire-Duct Electrostatic Precipitation Devices," *Journal of Applied Physics*, vol. 48, pp. 2231-2243, 1977.
[27] G. A. Kallio and D. E. Stock, "Computation of Electrical Conditions Inside Wire-Duct Electrostatic Precipitators Using a Combined Finite-Element, Finite-Difference Technique," *Journal of Applied Physics*, vol. 59, pp. 999-1005, 1985.
[28] F. W. Peek, *Dielectric Phenomenon in High Voltage Engineering*, McGraw-Hill, New York, 1966.
[29] F. C. Lai, P. J.Mckinney and J. H. Davidson, "Oscillatory Electrohydrodynamic Gas Flows," *Journal of Fluids Engineering*, vol. 117, pp. 491-497, 1995.
[30] F. C. Lai and S. S. Kulkarni, "Effects of Buoyancy on EHD-Enhanced Forced Convection in a Vertical Channel," *Journal of Thermophysics and Heat Transfer*, vol. 21, pp. 730-735, 2007.